© 2014. Published by The Company of Biologists Ltd | Development (2014) 141, 4479-4488 doi:10.1242/dev.116467

RESEARCH ARTICLE

Adipocyte amino acid sensing controls adult germline stem cell number via the amino acid response pathway and independently of Target of Rapamycin signaling in *Drosophila*

Alissa R. Armstrong[1,2], Kaitlin M. Laws[1,2] and Daniela Drummond-Barbosa[1,2,3,*]

ABSTRACT

How adipocytes contribute to the physiological control of stem cells is a critical question towards understanding the link between obesity and multiple diseases, including cancers. Previous studies have revealed that adult stem cells are influenced by whole-body physiology through multiple diet-dependent factors. For example, nutrient-dependent pathways acting within the *Drosophila* ovary control the number and proliferation of germline stem cells (GSCs). The potential role of nutrient sensing by adipocytes in modulating stem cells in other organs, however, remains largely unexplored. Here, we report that amino acid sensing by adult adipocytes specifically modulates the maintenance of GSCs through a Target of Rapamycin-independent mechanism. Instead, reduced amino acid levels and the consequent increase in uncoupled tRNAs trigger activation of the GCN2-dependent amino acid response pathway within adipocytes, causing increased rates of GSC loss. These studies reveal a new step in adipocyte-stem cell crosstalk.

KEY WORDS: Germline stem cells, Adipocytes, Amino acid transporters, Diet, Oogenesis, *Drosophila*

INTRODUCTION

Stem cell lineages are inextricably linked to whole-body physiology and nutrient availability in multiple organisms (Ables et al., 2012). For example, diet influences wound healing, hematopoietic transplants and cancer risk in humans, and evidence ranging from human epidemiological to model organism experimental data suggests that diet-dependent pathways impact a variety of adult stem cells (Ables et al., 2012). As intact living organisms vary their dietary input, multiple tissues and organs sense and respond to diet; however, our knowledge of how inter-organ communication contributes to the dietary control of adult stem cells remains limited.

The obesity epidemic has brought to light the crucial importance of normal adipocyte function in maintaining a healthy physiology. Adipocytes are highly sensitive to diet and produce long-range factors with key roles in metabolism, reproduction and other physiological processes (Rosen and Spiegelman, 2014). Conversely, dysfunctional adipocytes underlie the link between obesity and several diseases, including cancers (Vucenik and Stains, 2012). Whether sensing of dietary inputs by adipocytes leads to specific effects on adult stem cells in other organs, however, remains largely unexplored.

Drosophila female germline stem cells (GSCs) sense and respond to diet through complex endocrine mechanisms (Ables et al., 2012). Two or three GSCs reside within a well-defined niche in the germarium, the anterior region of the ovariole (Fig. 1A-C). Each asymmetric GSC division yields another GSC and a cystoblast that forms a 16-cell cyst, which is enveloped by follicle cells to generate a follicle that develops through oogenesis to form a mature oocyte (Spradling, 1993). On a yeast-rich diet, GSCs and their progeny grow and proliferate faster than on a yeast-free diet (Drummond-Barbosa and Spradling, 2001), and this response is mediated by diet-dependent factors that act on or within the ovary. For example, optimal levels of Target of Rapamycin (TOR) activity likely controlled by circulating amino acids are intrinsically required in GSCs for their proliferation and maintenance (LaFever et al., 2010; Sun et al., 2010). Insulin-like peptides produced by median neurosecretory cells in the brain act directly on GSCs to modulate how fast they proliferate to generate new cystoblasts (LaFever and Drummond-Barbosa, 2005; Hsu et al., 2008). In parallel, insulin-like peptides act directly on cap cells, the major cellular components of the niche, to control GSC maintenance via two mechanisms. Insulin-like peptides promote the response of cap cells to Notch ligands (Hsu and Drummond-Barbosa, 2009, 2011), which are required for proper cap cell numbers (Song et al., 2007), and also GSC-cap cell attachment via E-cadherin (Hsu and Drummond-Barbosa, 2009, 2011). These past studies, however, did not address whether or how nutrient sensing by adipocytes influences the dietary response of GSCs and their descendants.

Drosophila adipocytes, together with hepatocyte-like oenocytes, compose the fat body (Fig. 1A), a nutrient-sensing organ with endocrine roles (Colombani et al., 2003; Arrese and Soulages, 2010; Rajan and Perrimon, 2012). In the larval fat body, TOR activation downstream of amino acid sensing results in the production of unknown factors that modulate overall growth of the organism (Colombani et al., 2003). In both the larval and adult fat body, sensing of sugars and lipids leads to the production of a leptin-like cytokine, Unpaired 2 (Upd2), which controls the secretion of brain insulin-like peptides (Rajan and Perrimon, 2012). Here, we report that partially inhibiting amino acid transport in adult adipocytes results in a specific reduction in the number of ovarian GSCs and that, surprisingly, this effect is independent of TOR signaling. Instead, reduced amino acid levels and the consequent increase in uncoupled tRNAs trigger activation of the GCN2-dependent amino acid response (AAR) pathway within adipocytes, causing increased rates of GSC loss. These results indicate that amino acid sensing by adipocytes through a TOR-independent mechanism is communicated to GSCs to control their maintenance, thereby contributing to their response to diet. Our

[1]Department of Biochemistry and Molecular Biology, Bloomberg School of Public Health, Johns Hopkins University, Baltimore, MD 21205, USA. [2]Division of Reproductive Biology, Bloomberg School of Public Health, Johns Hopkins University, Baltimore, MD 21205, USA. [3]Department of Environmental Health Sciences, Bloomberg School of Public Health, Johns Hopkins University, Baltimore, MD 21205, USA.

*Author for correspondence (dbarbosa@jhu.edu)

Received 8 August 2014; Accepted 7 October 2014

Development (2014) 141, 4479-4488 doi:10.1242/dev.116467

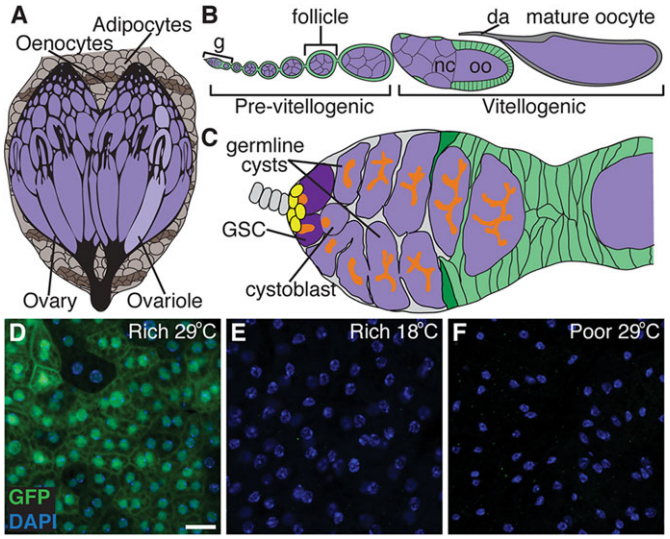

Fig. 1. A tool to determine how genetic manipulation of nutrient-dependent pathways in adult adipocytes impacts the GSC lineage in the *Drosophila* ovary. (A) The *Drosophila* fat body is an endocrine organ awash in hemolymph and composed of sheets of adipocytes intercalated with hepatocyte-like oenocytes. The fat body underlies the cuticle and surrounds the brain, gut and ovaries in females. (B) Developing follicles arranged in chronological order make up an ovariole. Follicles, formed in an anterior germarium (g), are germline cysts (one oocyte, oo, plus 15 nurse cells, nc; purple) surrounded by follicle cells (green), and develop to form a mature oocyte containing a dorsal appendage (da). (C) Each germarium contains two or three GSCs in a well-defined niche composed primarily of cap cells (yellow), and each GSC division yields a GSC and a cystoblast that forms a 16-cell cyst. GSCs and other early germline stages are identifiable based on the position and morphology of a germline-specific organelle, the fusome (orange). Follicle cells derived from follicle stem cells (dark green) envelop the cyst, making a follicle. (D-F) In females raised at 18°C and subsequently switched to 29°C, *Gal80^{ts}; Lsp2* drives *UAS* transgene expression specifically in adult adipocytes (see supplementary material Figs S1 and S2). A *UAS-GFP* reporter (green) driven by *Gal80^{ts}; Lsp2* shows robust expression in adipocytes on a rich diet at 29°C (D), but is not expressed either at 18°C (E) or on a poor diet (F). DAPI (blue) labels nuclei. Scale bar: 50 µm.

findings bring to light the importance of elucidating how adipocytes contribute to the regulation of various adult stem cell types by diet, and how these mechanisms might be adversely affected in obese individuals.

RESULTS

A tool for specific genetic manipulation of adult adipocytes

As a first step towards specific genetic manipulation of adult adipocytes using the *UAS/Gal4/Gal80* system (del Valle Rodriguez et al., 2012), we sought to identify a Gal4 driver that, in adults, shows expression exclusively in adipocytes. We tested several Gal4 drivers with previously reported expression in the larval and/or adult fat body (Fischer et al., 1988; Colombani et al., 2003; Gronke et al., 2003; Rusten et al., 2004; Lazareva et al., 2007; DiAngelo et al., 2009) using a *UAS-GFP* reporter. Most of these fat body drivers showed expression in at least one additional adult tissue on a yeast-rich diet (supplementary material Figs S1 and S2). By contrast, the *3.1Lsp2-Gal4* driver (Lazareva et al., 2007) drove robust GFP levels in adipocytes, with no detectable expression in oenocytes, brain, gut or ovaries (supplementary material Figs S1 and S2). Furthermore, by combining *3.1Lsp2-Gal4* with a temperature-sensitive *tub-Gal80^{ts}* transgene (McGuire et al., 2003) (*Gal80^{ts}; Lsp2*), we could temporally restrict its expression (Fig. 1D,E). In females raised at the permissive temperature (18°C), the active Gal80^{ts} protein inhibits Gal4 function and prevents GFP transgene expression (Fig. 1E). At the restrictive temperature (29°C), the Gal80^{ts} protein is inactive, allowing GFP expression exclusively in adult stages (Fig. 1D). Expression of *3.1Lsp2-Gal4*, however, was drastically decreased on a yeast-free diet (Fig. 1F), precluding the use of this driver under those conditions. Thus, *Gal80^{ts}; Lsp2* can be used as a tool to drive the expression of *UAS* transgenes specifically in adult adipocytes without interfering with development.

Decreased amino acid transport in adult adipocytes inhibits egg production

Amino acids are key dietary components that have systemic effects on organismal growth during development through their action in the larval fat body (Colombani et al., 2003). To test whether amino acid sensing in adipocytes might have an effect on the adult GSC lineage, we knocked down individual amino acid transporters in adult adipocytes using *Gal80^{ts}; Lsp2* and available *UAS-RNAi* lines (supplementary material Table S1, Fig. 2A). The *Drosophila* genome encodes 40 predicted amino acid transporters (www.flybase.org). Knockdown of single transporters in adult adipocytes did not lead to gross abnormalities in ovarian follicle development, fat body morphology or overall female health (Fig. 2B). For approximately one-third of the amino acid transporters tested, however, adipocyte-specific knockdown resulted in a significant decrease in the number of eggs laid (Fig. 3). These results suggest that incomplete loss of function of single transporters (and presumably relatively small changes in intracellular amino acid levels) within adipocytes are sufficient to influence oogenesis.

Reduced amino acid transport in adult adipocytes leads to increased GSC loss

Changes in GSC number or activity can contribute to alterations in egg production. We therefore determined whether GSCs are specifically affected by amino acid transport within adipocytes. Based on their pronounced egg laying reduction (Fig. 3) and reported fat body expression (supplementary material Table S1), we focused our analyses on females with adipocyte-specific knockdown of the amino acid transporters encoded by *CG12773*, *slimfast* (*slif*), *CG7708*, *CG1607*, *CG1628* and *CG13384*. The number of GSCs declined significantly faster over time in females with adipocyte amino acid transporter knockdown relative to controls (Fig. 4A; supplementary material Fig. S3), suggesting that reductions in amino acid levels within adipocytes can be communicated to the ovary to influence GSC maintenance.

GSC loss downstream of adipocyte amino acid sensing is not a consequence of severe niche impairment or of alterations in systemic insulin signaling

We next tested whether decreased amino acid levels in adipocytes cause GSC loss through reduced bone morphogenetic protein (BMP) signaling from the niche, which is required for GSC maintenance (Xie and Spradling, 1998). We measured the nuclear levels of phosphorylated Mad (pMad), a reporter of BMP signaling (Kai and Spradling, 2003), and found that GSCs in adipocyte transporter knockdown females showed variable levels of pMad (Fig. 4B,C). Specifically, there is a small (less than 50%) decrease in pMad levels for three amino acid transporters (encoded by *CG12773*, *CG13384* and *CG1607*), and an increase in those levels for the remaining transporters (*CG1628*, *slif* and *CG7708*). Even excluding *slif* and *CG7708* (for which sample sizes are small) from this analysis, there is no consistent and drastic decrease in pMad levels, even though all six transporters share the same reduced

Development (2014) 141, 4479-4488 doi:10.1242/dev.116467

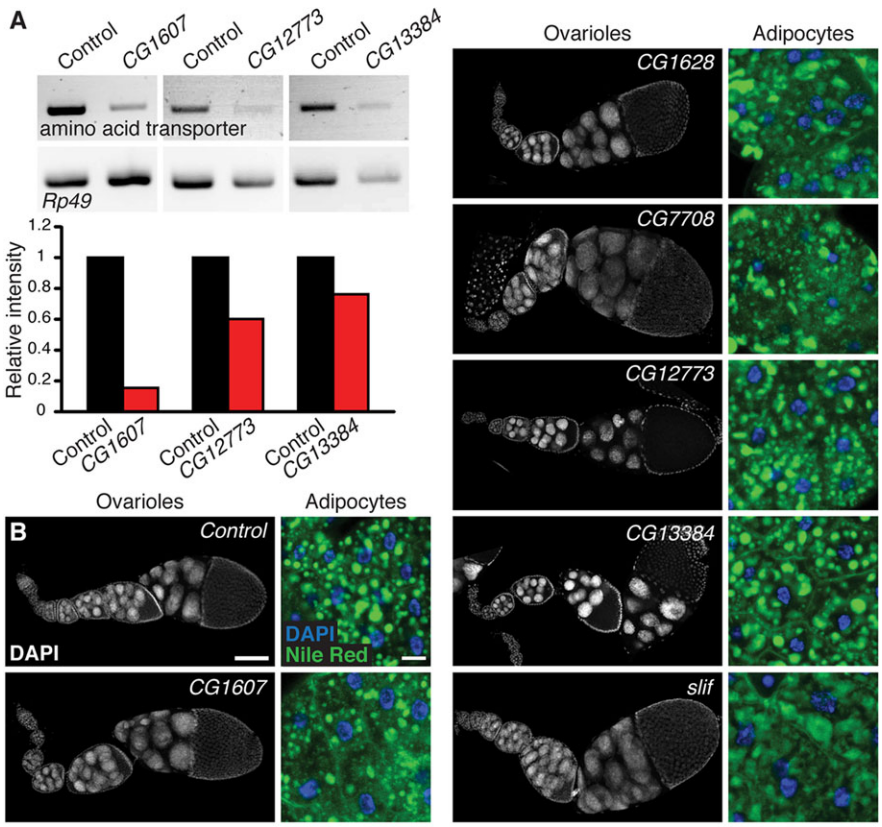

Fig. 2. Adult adipocyte-specific knockdown of amino acid transporters does not cause obvious changes in ovarian or adipocyte morphology. (A,B) RT-PCR analysis of hand-dissected fat bodies showing knockdown of amino acid transporters (A), and normal ovariole and adipocyte morphology (B) after 10 days of *Gal80^{ts}; Lsp2*-mediated induction of RNAi or antisense transgenes against amino acid transporters or *white* control. *Rp49* is a control. DAPI (white or blue) labels nuclei. In adipocytes, Nile Red, which fluoresces in both red and green (Greenspan et al., 1985), is shown in green. Scale bars: 100 µm (ovarioles); 10 µm (adipocytes).

GSC number phenotype. It is therefore unlikely that a severe impairment of BMP signaling is the cause of GSC loss, in agreement with the observation that adipocyte knockdown of *CG1628* shows a more severe GSC loss than knockdown of *CG13384*. We also did not observe dying cells adjacent to the GSC niche (Fig. 5A), suggesting that GSCs might be lost through differentiation, despite presumably adequate levels of BMP signaling.

During larval development, amino acid sensing by the fat body modulates systemic insulin signaling (Colombani et al., 2003), and our previous work showed that insulin-like peptides control GSC maintenance through the niche by controlling cap cell numbers and E-cadherin-mediated GSC-cap cell adhesion (Hsu and Drummond-Barbosa, 2009, 2011; Kwak et al., 2013). We therefore asked whether the reduction in GSC number resulting from amino acid transporter knockdown in adipocytes was due to changes in cap cell number or in E-cadherin levels. The numbers of cap cells, however, were unaltered (supplementary material Fig. S4A). Similarly, there were no obvious differences in the levels of E-cadherin at the niche-GSC junction (supplementary material Fig. S4B; number of germaria analyzed: 96 for control; 76 for *CG1607*; 15 for *CG1628*; 31 for *CG7708*; 74 for *CG12773*; 45 for *CG13384*; 69 for *slif*), although we cannot exclude the possibility of minor effects on E-cadherin levels based on this visual assessment. Also inconsistent with a general reduction in insulin signaling, GSC proliferation was increased and follicle cell division rates (a proxy for rates of follicle development) were unaltered or slightly increased in most cases upon amino acid transporter knockdown in adipocytes (Fig. 5B,C). Thus, reduced amino acid transport in adult adipocytes causes a specific decline in GSC numbers that is independent of changes in systemic insulin signaling or severe niche alterations.

General amino acid sensing in adult adipocytes does not affect vitellogenesis but appears to partially inhibit ovulation

To determine whether the GSC loss observed downstream of amino acid transporter knockdown in adipocytes is accompanied by additional alterations in the GSC lineage, we examined later stages of oogenesis. Onset of vitellogenesis and ovulation are major points of control of oogenesis by diet (Drummond-Barbosa and Spradling, 2001); therefore, we examined whether amino acid transport within adipocytes may also contribute to modulation of these processes. There was no increase in the percentage of ovarioles containing dying vitellogenic follicles upon adipocyte amino acid transporter knockdown, with the exception of *slif* antisense, which caused a small but significant increase in degeneration of vitellogenic follicles (supplementary material Fig. S5). These results are also consistent with normal levels of systemic insulin signaling, which are required for intact vitellogenesis (Drummond-Barbosa and Spradling, 2001; LaFever and Drummond-Barbosa, 2005; Hsu et al., 2008). By contrast, knockdown of several amino acid transporters resulted in a slight increase in the fraction of ovaries showing a partial block in the ovulation of mature oocytes relative to controls (Fig. 6A,B). The partial block in ovulation, however, was a variable phenotype that did not reach statistical significance, presumably owing to the mild decrease in amino acid transport expected from knockdown of individual transporters.

Adipocyte TOR signaling controls ovulation but does not mediate the effects of adipocyte amino acid sensing on GSC maintenance

The nutrient sensor TOR acts downstream of Slif within larval adipocytes to promote organismal growth (Colombani et al., 2003), prompting us to ask whether adipocyte TOR signaling mediates the effects of amino acid transporters within adult adipocytes on the

Development (2014) 141, 4479-4488 doi:10.1242/dev.116467

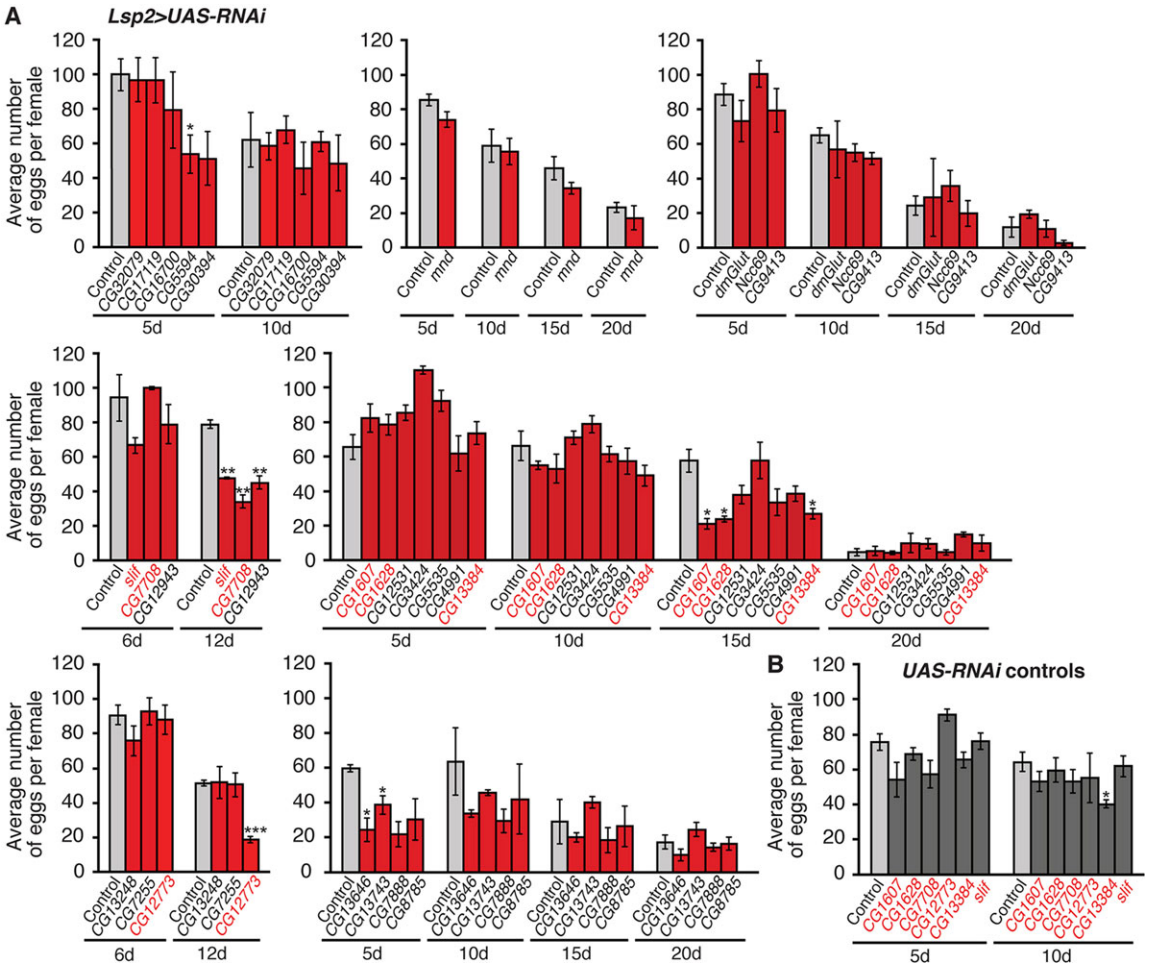

Fig. 3. Adult adipocyte-specific knockdown of a subset of amino acid transporters encoded by *slif*, *CG7708*, *CG1607*, *CG13384*, *CG1628* and *CG12773* results in reduced egg production. (A) Females carrying *Gal80^{ts}; Lsp2* and *UAS-RNAi* transgenes against amino acid transporters [or a *UAS*-antisense transgene (Colombani et al., 2003) in the case of *slif*] or a control *UAS-RNAi* (against *white*, an eye color gene) raised at 18°C and switched to 29°C for adult adipocyte-specific knockdown for the indicated number of days. Knockdown of a subset of transporters causes a significant decrease in the average number of eggs laid per female per day. Transporters in red font were followed up on in this study. (B) Control females carrying *UAS-RNAi* or -antisense transgenes against amino acid transporters in the absence of *Gal80^{ts}; Lsp2* and subjected to the same temperature regime as in A show egg-laying rates that are statistically indistinguishable from those of a *UAS-GFP^{RNAi}* control, except for *UAS-CG13384^{RNAi}*. *P<0.05; **P<0.01; ***P<0.001, Student's *t*-test. Data shown as mean±s.e.m.

ovarian GSC lineage. We inhibited TOR signaling specifically within adult adipocytes using *Gal80^{ts}; Lsp2*-driven overexpression of the Tuberous Sclerosis Complex (Tsc)1/Tsc2 complex (Tapon et al., 2001) [a negative regulator of TOR (Laplante and Sabatini, 2012)] or of a dominant-negative version of RagA [RagA^{T16N} (Kim et al., 2008)], a positive regulator of TOR involved in amino acid sensing (Laplante and Sabatini, 2012). Inhibition of adipocyte TOR signaling using either of these established tools caused a marked increase in the percentage of ovaries showing a partial block in ovulation relative to controls (Fig. 6A,B). Adipocyte TOR inhibition, however, had no effect on GSC (or cap cell) numbers (Fig. 6C, supplementary material Fig. S6), suggesting that adipocyte amino acid levels control GSC maintenance independently of TOR signaling.

Increased levels of unloaded tRNAs and GCN2 activation in response to reduced amino acid levels in adipocytes cause GSC loss

We next hypothesized that the AAR pathway may act within adipocytes to control GSC numbers. The AAR pathway, conserved from yeast to mammals, senses limitations in one or more amino acids. Reduced amino acid levels lead to an increase in unloaded tRNAs, which activate the kinase GCN2, thereby controlling downstream translational and transcriptional events (Gietzen and Rogers, 2006; Gallinetti et al., 2013; Bjordal et al., 2014). Our hypothesis therefore predicts that directly increasing unloaded tRNA levels in adipocytes should reduce GSC numbers. Inhibiting or mutating aminoacyl-tRNA synthetases (the enzymes responsible for coupling amino acids to their cognate tRNAs) are well-established approaches to experimentally increase uncharged tRNA levels, thereby activating the AAR pathway under normal amino acid levels (Gietzen and Rogers, 2006; Gallinetti et al., 2013). Given that Slif, a cationic amino acid transporter (Colombani et al., 2003), is among those that function in adipocytes to control GSC numbers (see Fig. 4A), we knocked down the genes encoding Histidyl-, Arginyl- or Lysyl-tRNA synthetases (*Aats-his*, *Aats-arg* or *Aats-lys*, respectively) in adipocytes using *Gal80^{ts}; Lsp2* (supplementary material Fig. S7). Control or *Aats-lys* adipocyte knockdown (which was relatively inefficient; supplementary material Fig. S7C) had no effect on GSC number. By contrast, knockdown of aminoacyl-tRNA synthetases using either an

Development (2014) 141, 4479-4488 doi:10.1242/dev.116467

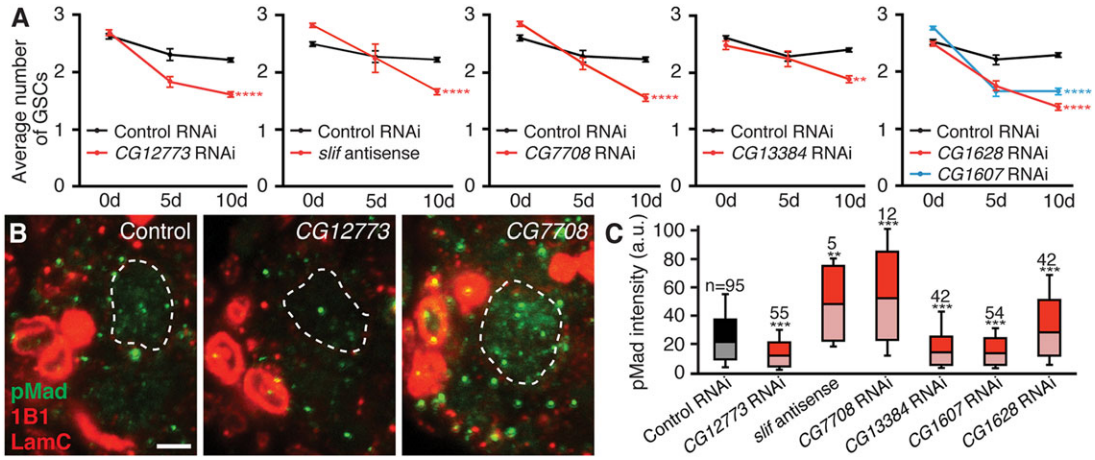

Fig. 4. Adult adipocyte-specific knockdown of amino acid transporters leads to increased rates of GSC loss in the ovary. (A) Average number of GSCs per germarium at 0, 5 or 10 days of *Gal80^{ts}; Lsp2*-mediated induction of RNAi or antisense transgenes against amino acid transporters or *white* control. See supplementary material Fig. S3 for sample sizes and distribution. ***P*<0.01; *****P*<0.0001, two-way ANOVA with interaction. Data shown as mean±s.e.m. (B) Germaria at 10 days of adipocyte-specific *GFP* control or amino acid transporter RNAi labeled for phosphorylated Mad (pMad; green), 1B1 (red, fusome) and Lamin C (red, cap cell nuclear envelope). GSC nuclei are outlined. Scale bar: 2.5 µm. (C) Box and whisker plot of mean nuclear pMad intensity for experiment in B. Sample sizes are included above. ***P*<0.01; ****P*<0.001, Student's *t*-test.

Aats-his or two distinct *Aats-arg* RNAi transgenes in adipocytes led to a marked decrease in GSC number upon transgene induction (Fig. 7A, supplementary material Fig. S7A). Similar to what we observed for amino acid transporter knockdown, there were no changes in cap cell number (supplementary material Fig. S7B). These results show that activation of the AAR pathway suffices to phenocopy the GSC loss caused by reduced amino acid transport in adipocytes. Conversely, adipocyte-specific knockdown of *Gcn2* reverts the GSC loss caused by RNAi of the amino acid transporter *CG12773* (Fig. 7B,C), further suggesting that the AAR pathway is also required to mediate the effects of adipocyte amino acid transporters on GSCs. Based on these results, we conclude that the

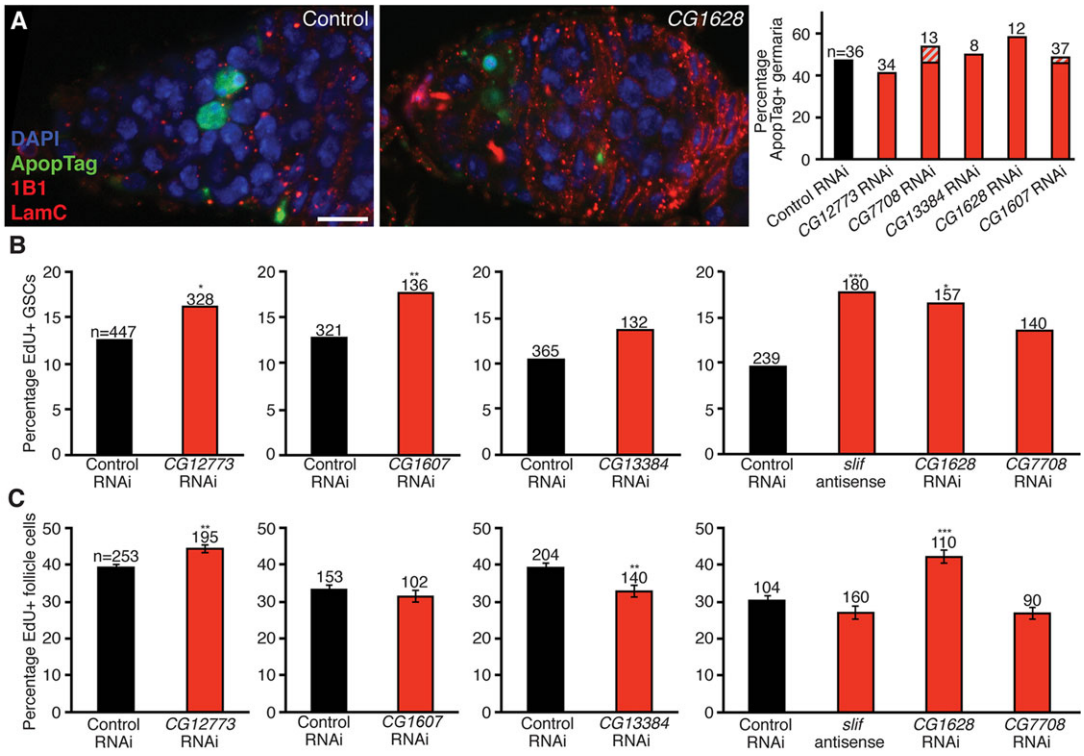

Fig. 5. Reduced amino acid transport in adipocytes does not affect cell death within the germarium, but causes a slight increase in GSC proliferation. (A) Germaria from females at 10 days of adult adipocyte-specific knockdown of *CG1628* or *white* control showing some occurrence of cell death (ApopTag, green) in both cases. DAPI (blue) labels nuclei; 1B1 (red) labels fusomes; LamC (red) labels cap cell nuclear envelopes. Scale bar: 10 µm. In the graph on right, bars represent the percentage of germaria containing ApopTag-positive cells, with the hatched region indicating the fraction of those displaying ApopTag adjacent to GSC niche. The number of germaria analyzed is shown above each bar. (B,C) Frequencies of GSCs (B) or follicle cells (C) in S phase, based on EdU incorporation, at 10 days of adipocyte knockdown of amino acid transporters or *GFP* control. Number of GSCs (B) or follicle cell fields (C) analyzed is shown above each bar. **P*<0.05; ***P*<0.01; ****P*<0.001, Student's *t*-test. Data shown as mean±s.e.m.

Development (2014) 141, 4479-4488 doi:10.1242/dev.116467

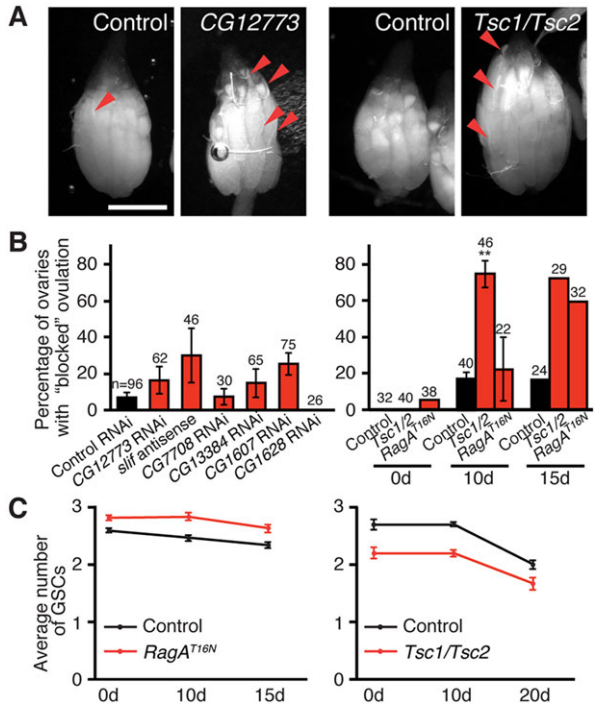

Fig. 6. GSC loss induced by adult adipocyte-specific knockdown of amino acid transporters is independent of TOR signaling. (A) Ovaries at 10 days of adipocyte-specific *CG12773* knockdown or *Tsc1*/*Tsc2* induction showing retention of mature oocytes in subsets of ovarioles ('blocked' ovulation). Mature oocytes are recognizable by the presence of dorsal appendages (arrowheads). Scale bar: 500 µm. (B) Percentage of ovaries containing at least one ovariole that retains more than one mature oocyte at 10 days of adipocyte-specific amino acid transporter knockdown (left) or at different days of inhibition of TOR signaling (right). $^{**}P<0.01$. Data from 0 d and 15 d time points are from one experiment, whereas 10 d represents three experiments. Number of ovaries analyzed is shown above each bar. (C) Average number of GSCs at different days of $Gal80^{ts}$; *Lsp2*-mediated induction of a dominant-negative *RagA* ($RagA^{T16N}$) or of *Tsc1*/*Tsc2* transgenes showing that inhibition of TOR signaling has no effect on GSC maintenance. See supplementary material Fig. S6 for sample sizes and distribution. Control is *GFP* RNAi for A and B (left), and $Gal80^{ts}$; *Lsp2* alone for B (right) and C.

AAR pathway within adipocytes is sufficient and required to initiate an amino acid-dependent signaling cascade of inter-organ communication to modulate GSC maintenance in the ovary.

DISCUSSION

The specific effects of adipocyte dysfunction on normal stem cell lineages have remained largely unexplored. Yet, clear evidence shows that obesity leads to higher risk for multiple chronic diseases (Vucenik and Stains, 2012). Our data support the model that amino acid levels within adipocytes are sensed through separate mechanisms that specifically affect a stem cell lineage at distinct stages (Fig. 7D). The AAR pathway acting within adipocytes influences maintenance of GSCs, whereas amino acid sensing through the adipocyte Rag/TOR pathway modulates the efficiency of ovulation of fully differentiated GSC daughters, or oocytes. Future studies should identify the extracellular factors acting downstream of these intra-adipocyte signaling cascades to communicate adipocyte nutritional status to the GSC lineage. This work underscores the importance of investigating the role of inter-organ communication in the control of stem cells and their differentiated daughters in a wide variety of systems. Furthermore, it suggests that the aberrant co-option of endocrine pathways that normally tie stem cell lineages to whole-body physiology might contribute to the increased cancer risk associated with obesity (Vucenik and Stains, 2012).

Drosophila as a model for investigating how inter-organ communication contributes to the regulation of adult stem cells

Drosophila is an ideal model for molecular physiology studies, owing to the ease of cell/tissue-specific manipulations (del Valle Rodriguez et al., 2012), which are essential to dissect how individual systemic signaling events contribute to complex physiological networks. Indeed, recent years have seen an explosion in metabolism and physiology studies using *Drosophila* (Colombani et al., 2003, 2012; Gutierrez et al., 2007; Arquier et al., 2008; Geminard et al., 2009; Palanker et al., 2009; Sieber and Thummel, 2009; Slaidina et al., 2009; Delanoue et al., 2010; Ruaud et al., 2011). Particularly useful throughout these studies is the *UAS/Gal4* system, which allows tissue- and/or cell-type-specific genetic manipulations; however, a crucial consideration when designing such studies is the specificity of *Gal4* expression to avoid misinterpretation of phenotypes. Indeed, most of the published fat body drivers we tested were not expressed exclusively in adipocytes in adult females. By contrast, the robust and highly specific expression of *3.1Lsp2-Gal4* in adipocytes makes it a valuable tool for exclusive genetic manipulation of adipocytes to test how they impact not only GSCs, but also other adult stem cell types.

In addition to adipocytes, nutrient sensing by other tissues also affects GSCs. For example, insulin-like peptides secreted from the brain act directly on the germline to modulate GSC proliferation, cyst growth and vitellogenesis, and also indirectly affect GSC maintenance through effects on the niche (LaFever and Drummond-Barbosa, 2005; Hsu and Drummond-Barbosa, 2009, 2011). Other adult stem cell types are also modulated by insulin signaling, including male GSCs and intestinal stem cells (Ables et al., 2012). Much remains unknown, however, about how other tissues influence stem cells, despite evidence suggesting endocrine roles for muscle (O'Brien et al., 2011; Demontis et al., 2014), intestines (Reiher et al., 2011) and the brain (Nassel and Winther, 2010).

Separate modes of amino acid sensing in adipocytes affect the stem cell lineage at distinct stages

Our findings that amino acid sensing by adipocytes controls GSC maintenance through the AAR pathway and ovulation through TOR clearly illustrate the high degree of specificity of adipocyte-to-ovary communication. Our results also imply that relatively small fluctuations in amino acid levels (e.g. those resulting from partial knockdown of single amino acid transporters) within adipocytes can be effectively transmitted to the ovary to modulate stem cell number. These same slight reductions in amino acid levels resulted in less significant effects on ovulation, consistent with the distinct amino acid sensing mechanisms involved. It will be very interesting to identify and study the effectors downstream of AAR and TOR signaling that mediate these distinct effects on the GSC lineage.

Not surprisingly, inhibition of TOR signaling impacted ovulation more severely than manipulation of single amino acid transporters, in agreement with its role downstream of transporters and as an integrator of multiple inputs, including nutrients, energy status and growth factors (Dibble and Manning, 2013). It is likely that additional stimuli upstream of TOR within adipocytes also regulate ovulation.

Development (2014) 141, 4479-4488 doi:10.1242/dev.116467

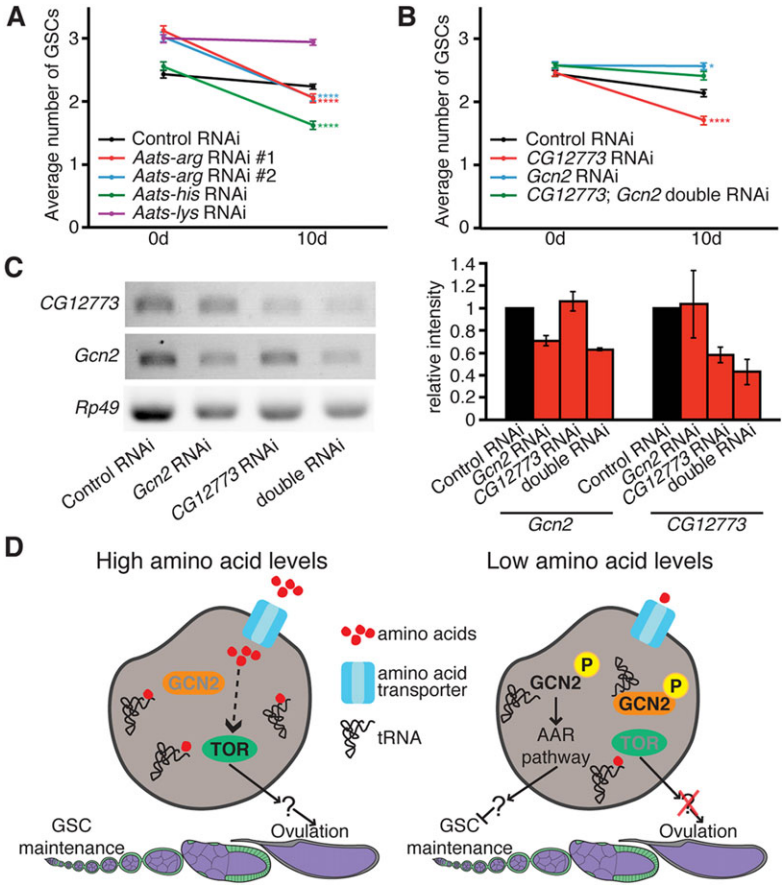

Fig. 7. The amino acid response pathway within adipocytes contributes to the control of GSC maintenance. (A,B) Average number of GSCs at 0 or 10 days of *Gal80^{ts}; Lsp2*-mediated induction of *GFP* control, *Arginyl-tRNA synthetase* (*Aats-arg*), *Histidyl-tRNA synthetase* (*Aats-his*), *Lysyl-tRNA synthetase* (*Aats-lys*), *CG12773*, *Gcn2* and double *CG12773 Gcn2* RNAi transgenes. See supplementary material Fig. S7 for sample sizes and distribution, and for efficiency of knockdown for experiment in A. Numbers of germaria analyzed in B are: 131 for control 0 d; 71 for control 10 d; 121 for *CG12773* 0d; 89 for *CG12773*; 121 for *Gcn2* 0 d; 102 for *Gcn2* 10 d; 159 for *CG12773 Gcn2* double 0 d; 90 for *CG12773 Gcn2* double 10 d. *P<0.05; ****$P\leq$0.0001, two-way ANOVA with interaction. Data are mean±s.e.m. (C) RT-PCR analysis of hand-dissected fat bodies showing specific knockdown of *Gcn2* and/or *CG12773* in genotypes shown in B. Data shown as mean±s.e.m. (D) Model for how amino acid sensing within adipocytes regulates the GSC lineage. Under high amino acid levels, the amino acid response (AAR) pathway is off and TOR is active, resulting in optimal GSC maintenance and ovulation rates. Under lower amino acid levels, the AAR pathway is triggered through an increase in unloaded tRNAs and activation of GCN2 kinase, leading to GSC loss. Reduced TOR activity causes a partial block in ovulation.

Context-specific targets of the amino acid response pathway

The AAR pathway is evolutionarily conserved from yeast to humans; however, its downstream targets are context dependent. In yeast, for example, phosphorylation of eIF2α by activated GCN2 causes selective upregulation of translation of the transcriptional factor GCN4, which in turn induces genes involved in amino acid transport as well as in amino acid biosynthesis (Natarajan et al., 2001). Translational derepression of ATF4 (the GCN4 equivalent in *Drosophila* and humans), by contrast, leads to expression of oxidative stress genes in mouse embryonic fibroblasts (Harding et al., 2003). The targets of the AAR pathway in the context of intact multicellular organisms remain largely unidentified. Nevertheless, it is reasonable to speculate that the sets of targets regulated by the AAR pathway in different tissues and cell types may be quite different, given the diversity of processes being modulated. For example, the AAR pathway acts in the brains of *Drosophila* larvae, mice and rats to reduce intake of food sources that lack essential amino acids (Hao et al., 2005; Gietzen and Rogers, 2006; Bjordal et al., 2014). Our study demonstrates a starkly different role of the AAR pathway in adipocytes in the control of GSC numbers. A fascinating challenge for future studies will be to identify the subsets of targets activated in a cell-type, context-dependent manner, and to investigate how the specificity of this pathway is achieved from budding yeast to *Drosophila* adipocytes to *Drosophila* and rodent neurons to achieve such differing cellular outcomes. Our studies raise the possibility that specific targets downstream of ATF4 induced in adipocytes signal to the ovary to control GSC number. Additional studies in different tissues and conditions will elucidate how much overlap exists of targets induced by the AAR pathway. Finally, it is also possible that activation of the AAR pathway in adipocytes in response to increased levels of unloaded tRNAs could alter signals from adipocytes to GSCs downstream of either global reduction in translation or of increased levels of ATF4 and its targets (Murguia and Serrano, 2012).

Adipocytes, stem cells and increased cancer risk in obese individuals

Obesity and high calorie intake are associated with increased risk of multiple cancer types, including breast, colon and prostate cancer (Bianchini et al., 2002; McMillan et al., 2006; Xue and Michels, 2010). Similar to GSCs and other stem cells (Ables et al., 2012), cancers are highly responsive to nutrient-sensing pathways, and components of the insulin and TOR pathways are often misregulated in cancers (Jee et al., 2005; Chen, 2011). Given the parallels between cancer cells and stem cells, investigations of the role of adipocytes in adult stem cell regulation will likely provide valuable insights into the link between obesity and cancer risk. Based on our results, we speculate that aberrant communication of the nutrient-sensing status of fat cells could modulate the activity of cancer cells and might explain the link between diet, adiposity and cancer.

MATERIALS AND METHODS

Drosophila strains and culture conditions

Fly stocks were maintained at 22-25°C on standard medium containing cornmeal, molasses, yeast and agar. Standard medium supplemented with wet yeast paste was used for all experiments, except for Fig. 1F, where flies were kept on molasses/agar plates with no yeast. Previously described fat body Gal4 lines were used: *Adh-Gal4* (Fischer et al., 1988), *cg-Gal4* (Rusten et al., 2004), *FB-Gal4* (Gronke et al., 2003), *r4-Gal4* (DiAngelo et al., 2009), *pumpless-Gal4* (Colombani et al., 2003) and *3.1Lsp2-Gal4* (Lazareva et al., 2007). The temperature-sensitive *tub-Gal80^{ts}* transgene has been described (McGuire et al., 2003). *UAS-RNAi* lines obtained from the

Development (2014) 141, 4479-4488 doi:10.1242/dev.116467

Vienna *Drosophila* RNAi Stock Center (http://stockcenter.vdrc.at) and the Transgenic RNAi Project (http://www.flyrnai.org) collection at Bloomington Drosophila Stock Center (http://flystocks.bio.indiana.edu) for knockdown of amino acid transporters are listed in supplementary material Table S1. Other *UAS-RNAi* lines used were: *P{GD14098}v42184* (line 1) and *P{GD14098}v42185* (line 2), against *Aats-arg*; *P{KK102374}VIE-260B*, against *Aats-his*; *P{TRiP.HMS00763}attP2*, against *Aats-lys*; *P{TRiP.GL00267}attP2*, against *Gcn2*; *P{UAS-GFP.dsRNA.R}143*, against *GFP* (used as a control); *P{TRiP.JF01545}attP2*, and against *white* (used as a control). The *UAS-CG12773^{RNAi}; UAS-Gcn2^{RNAi}* and *tub-Gal80^{ts}; 3.1Lsp2-Gal4* (*Gal80^{ts}; Lsp2*) lines were generated by standard crosses. The following *UAS* lines have been described previously: *UAS-slif* antisense (Colombani et al., 2003), *UAS-Tsc1; UAS-Tsc2* (Tapon et al., 2001) and *UAS-RagA^{T16N}* (Kim et al., 2008). Other genetic elements used are described in FlyBase (http://www.flybase.org).

Adult adipocyte-specific genetic manipulations

For adult adipocyte-specific genetic manipulation, females of genotypes *yw; tub-Gal80^{ts}/+; 3.1Lsp2-Gal4/UAS-X* or *yw; tub-Gal80^{ts}/UAS-X; 3.1Lsp2-Gal4/+* were used. (*UAS-X* represents any of the *UAS* transgenes in this study.) Females were raised at 18°C, the permissive temperature for Gal80^{ts}, to keep transgene expression off during development. Newly eclosed females were maintained at 18°C for 3 days and then switched to 29°C, the restrictive temperature for Gal80^{ts}, for various lengths of time to induce transgene expression prior to dissection and/or analyses.

Immunostaining and fluorescence microscopy

All tissues were dissected in Grace's medium (BioWhittaker) and fixed in 5.3% formaldehyde (Ted Pella) in Grace's medium at room temperature for the following amounts of time: 13 min for ovaries, 20 min for abdominal carcasses (containing attached fat body) or brains, and 1 h for guts. Tissues were rinsed and washed three times in 0.1% Triton X-100 (Sigma) in phosphate-buffered saline (PBS), or PBT, and subsequently blocked in 5% bovine serum albumin (BSA; Sigma) and 5% normal goat serum (NGS; Jackson ImmunoResearch) in PBT, or blocking solution, for 3 h at room temperature or overnight at 4°C. Tissues were incubated overnight at 4°C in the following primary antibodies diluted in blocking solution: rabbit anti-GFP (Torrey Pines; 1:2500, TP401); mouse monoclonal anti-Hts (1B1) (DSHB; 1:10); mouse anti-α-spectrin (3A9) (DSHB; 1:50); mouse monoclonal anti-Lamin C (LC28.26) (DSHB; 1:100); rat monoclonal anti-E-cadherin (DCAD2) (DSHB; 1:100); and rabbit anti-pMad (Smad3) (Epitomics; 1:100, #1880). [This particular Smad3 antibody is widely used in *Drosophila* to detect pMad specifically (Hayashi et al., 2009; Ables and Drummond-Barbosa, 2010; Issigonis and Matunis, 2012; Matsuoka et al., 2013; Ma et al., 2014; Sulkowski et al., 2014).] Tissues were washed in PBT, and incubated for 2 h at room temperature in 1:200 Alexa Fluor 488- or 568-conjugated secondary antibodies (Molecular Probes). Samples were washed, and ovaries, brains, guts and fat bodies (scraped off from carcasses) were mounted in Vectashield containing DAPI (Vector Labs). For visualization of lipid droplets, fixed and blocked carcasses were incubated in 1:200 Nile Red (Sigma) in 50% glycerol in PBS for 10 min at room temperature. Fat bodies were mounted in 90% glycerol in PBS containing 0.5 µg/ml DAPI (Sigma). Data were collected with a Zeiss AxioImager-A2 fluorescence microscope or a Zeiss LSM700 confocal microscope. For nuclear pMad quantification, the densitometric mean of individual GSC nuclei was measured from optical sections containing the largest nuclear diameter (visualized by DAPI) using AxioVision. (To achieve as much consistency as possible among samples for pMad measurements, ovaries were dissected, fixed and stained in parallel under identical conditions, and the image acquisition settings were exactly the same for all images used for quantification.)

GSC and cap cell analyses

Cap cells were identified based on their ovoid shape and Lamin C staining, and GSCs were identified based on their juxtaposition to cap cells and fusome morphology and position, as described previously (Hsu et al., 2008; Hsu and Drummond-Barbosa, 2009). For statistical analysis of differences in rates of GSC loss we used two-way ANOVA with interaction (www.graphpad.com), which, simply stated, calculates the significance of any differences measured among genotypes in how much GSC numbers change over time.

Egg counts and ovulation analyses

To measure egg production, five pairs of flies (females of appropriate genotype and *y w* wild-type males) were maintained in plastic bottles containing molasses/agar plates covered by a thin layer of wet yeast paste, in triplicate, at 29°C. Plates were replaced daily, and eggs laid within the preceding 24 h were counted on specific days throughout experiments.

For ovulation analyses, females were dissected in Grace's medium and intact ovaries were examined under a Zeiss Stemi 2000 stereomicroscope. Each ovariole in a wild-type ovary typically contains zero or one mature oocyte, recognizable by its fully developed dorsal appendage (Spradling, 1993). Ovaries in which at least one ovariole contained two or more mature oocytes were classified as having partially blocked ovulation. Images of whole ovaries were captured using a Nikon Coolpix L620 digital camera.

EdU incorporation, apoptosis assay and quantification of vitellogenesis defects

For EdU analysis, intact ovaries were incubated for 1 h at room temperature in 100 µM EdU (Molecular Probes) diluted in Grace's medium, washed, fixed as described and permeabilized for 20 min in 0.5% Triton X-100 in PBS. Following primary antibody incubation, EdU samples were subjected to the Click-iT reaction according to the manufacturer's protocol (Life Technologies) for 30 min at room temperature. GSC proliferation rates were determined by calculating the fraction of EdU-positive GSCs as a percentage of the total number of GSCs analyzed per genotype. To measure follicle cell proliferation, single confocal planes transecting follicle monolayers (i.e. follicle cell fields) at the top and bottom of flatly mounted ovarioles were acquired, and the average percentage of EdU-positive follicle cells per follicle cell field was calculated. This analysis included follicle cells covering follicle stages 4 to 6, prior to the mitotic-to-endoreplication switch, as described previously (LaFever et al., 2010).

ApopTag Direct *In Situ* Apoptosis Detection Kit (Millipore) was used as described (Drummond-Barbosa and Spradling, 2001). Progression through vitellogenesis was assessed using DAPI staining (Spradling, 1993). Ovarioles containing vitellogenic follicles were easily distinguished from those with blocked vitellogenesis, which contained at least one dying vitellogenic follicle. Dying vitellogenic follicles were recognizable by their position within the ovariole and by the presence of pyknotic nuclei.

RT-PCR analyses

Fat bodies from 2-10 females per genotype at 10 days of RNAi induction were hand dissected in RNAlater solution (Ambion). RNA was extracted using the RNAqueous-4PCR DNA-free RNA Isolation for RT-PCR kit (Ambion) and cDNA was synthesized using the SSRII kit (Ambion) according to the manufacturer's protocols. For each primer pair, PCR was performed on both the control and corresponding RNAi samples. The primers used are listed in supplementary material Table S2. *Rp49* primers were used as a control. Band intensity was quantified using AxioVision by subtracting background pixels from band pixels in a fixed size box (net band intensity) and normalized to the net band intensity of the corresponding *Rp49* band. Controls were set to one and experimental sample intensities were determined relative to control.

Acknowledgements

We thank B. Cauwalder, P. Leopold, I. Hariharan, J. Bateman, T. Neufeld, R. Kühnlein, the Bloomington Stock Center, the Vienna *Drosophila* RNAi Stock Center, the TRiP at Harvard Medical School and the Developmental Studies Hybridoma Bank for fly stocks and reagents. We also thank C. Thompson at the Johns Hopkins Biostatistics Center for assistance with statistical analysis, K. Bois for technical support, and P. Coulombe for use of digital camera.

Competing interests

The authors declare no competing financial interests.

Author contributions
A.R.A. and D.D.-B. designed the experiments and wrote the manuscript. A.R.A. and K.M.L. performed the experiments. A.R.A., K.M.L. and D.D.-B. interpreted the experiments.

Funding
Supported by National Institutes of Health (NIH) [R01 GM 069875]. A.R.A. and K.M.L. were supported by an NIH training grant [T32 CA 009110]. A.R.A. was also supported by a National Research Service Award [F32 GM 106718] from the NIH. Deposited in PMC for release after 12 months.

Supplementary material
Supplementary material available online at
http://dev.biologists.org/lookup/suppl/doi:10.1242/dev.116467/-/DC1

References

Ables, E. T. and Drummond-Barbosa, D. (2010). The steroid hormone ecdysone functions with intrinsic chromatin remodeling factors to control female germline stem cells in Drosophila. *Cell Stem Cell* **7**, 581-592.
Ables, E. T., Laws, K. M. and Drummond-Barbosa, D. (2012). Control of adult stem cells in vivo by a dynamic physiological environment: diet-dependent systemic factors in Drosophila and beyond. *Wiley Interdiscip. Rev. Dev. Biol.* **1**, 657-674.
Arquier, N., Géminard, C., Bourouis, M., Jarretou, G., Honegger, B., Paix, A. and Léopold, P. (2008). Drosophila ALS regulates growth and metabolism through functional interaction with insulin-like peptides. *Cell Metab.* **7**, 333-338.
Arrese, E. L. and Soulages, J. L. (2010). Insect fat body: energy, metabolism, and regulation. *Annu. Rev. Entomol.* **55**, 207-225.
Bianchini, F., Kaaks, R. and Vainio, H. (2002). Overweight, obesity, and cancer risk. *Lancet Oncol.* **3**, 565-574.
Bjordal, M., Arquier, N., Kniazeff, J., Pin, J. P. and Léopold, P. (2014). Sensing of amino acids in a dopaminergic circuitry promotes rejection of an incomplete diet in Drosophila. *Cell* **156**, 510-521.
Chen, J. (2011). Multiple signal pathways in obesity-associated cancer. *Obes. Rev.* **12**, 1063-1070.
Colombani, J., Raisin, S., Pantalacci, S., Radimerski, T., Montagne, J. and Léopold, P. (2003). A nutrient sensor mechanism controls Drosophila growth. *Cell* **114**, 739-749.
Colombani, J., Andersen, D. S. and Leopold, P. (2012). Secreted peptide Dilp8 coordinates Drosophila tissue growth with developmental timing. *Science* **336**, 582-585.
del Valle Rodríguez, A., Didiano, D. and Desplan, C. (2012). Power tools for gene expression and clonal analysis in Drosophila. *Nat. Methods* **9**, 47-55.
Delanoue, R., Slaidina, M. and Léopold, P. (2010). The steroid hormone ecdysone controls systemic growth by repressing dMyc function in Drosophila fat cells. *Dev. Cell* **18**, 1012-1021.
Demontis, F., Patel, V. K., Swindell, W. R. and Perrimon, N. (2014). Intertissue control of the nucleolus via a myokine-dependent longevity pathway. *Cell Rep.* **7**, 1481-1494.
DiAngelo, J. R., Bland, M. L., Bambina, S., Cherry, S. and Birnbaum, M. J. (2009). The immune response attenuates growth and nutrient storage in Drosophila by reducing insulin signaling. *Proc. Natl. Acad. Sci. USA* **106**, 20853-20858.
Dibble, C. C. and Manning, B. D. (2013). Signal integration by mTORC1 coordinates nutrient input with biosynthetic output. *Nat. Cell Biol.* **15**, 555-564.
Drummond-Barbosa, D. and Spradling, A. C. (2001). Stem cells and their progeny respond to nutritional changes during Drosophila oogenesis. *Dev. Biol.* **231**, 265-278.
Fischer, J. A., Giniger, E., Maniatis, T. and Ptashne, M. (1988). GAL4 activates transcription in Drosophila. *Nature* **332**, 853-856.
Gallinetti, J., Harputlugil, E. and Mitchell, J. R. (2013). Amino acid sensing in dietary-restriction-mediated longevity: roles of signal-transducing kinases GCN2 and TOR. *Biochem. J.* **449**, 1-10.
Géminard, C., Rulifson, E. J. and Léopold, P. (2009). Remote control of insulin secretion by fat cells in Drosophila. *Cell Metab.* **10**, 199-207.
Gietzen, D. W. and Rogers, Q. R. (2006). Nutritional homeostasis and indispensable amino acid sensing: a new solution to an old puzzle. *Trends Neurosci.* **29**, 91-99.
Greenspan, P., Mayer, E. P. and Fowler, S. D. (1985). Nile red: a selective fluorescent stain for intracellular lipid droplets. *J. Cell Biol.* **100**, 965-973.
Grönke, S., Beller, M., Fellert, S., Ramakrishnan, H., Jäckle, H. and Kühnlein, R. P. (2003). Control of fat storage by a Drosophila PAT domain protein. *Curr. Biol.* **13**, 603-606.
Gutierrez, E., Wiggins, D., Fielding, B. and Gould, A. P. (2007). Specialized hepatocyte-like cells regulate Drosophila lipid metabolism. *Nature* **445**, 275-280.
Hao, S., Sharp, J. W., Ross-Inta, C. M., McDaniel, B. J., Anthony, T. G., Wek, R. C., Cavener, D. R., McGrath, B. C., Rudell, J. B., Koehnle, T. J. et al. (2005). Uncharged tRNA and sensing of amino acid deficiency in mammalian piriform cortex. *Science* **307**, 1776-1778.
Harding, H. P., Zhang, Y., Zeng, H., Novoa, I., Lu, P. D., Calfon, M., Sadri, N., Yun, C., Popko, B., Paules, R. et al. (2003). An integrated stress response regulates amino acid metabolism and resistance to oxidative stress. *Mol. Cell* **11**, 619-633.
Hayashi, Y., Kobayashi, S. and Nakato, H. (2009). Drosophila glypicans regulate the germline stem cell niche. *J. Cell Biol.* **187**, 473-480.
Hsu, H.-J. and Drummond-Barbosa, D. (2009). Insulin levels control female germline stem cell maintenance via the niche in Drosophila. *Proc. Natl. Acad. Sci. USA* **106**, 1117-1121.
Hsu, H.-J. and Drummond-Barbosa, D. (2011). Insulin signals control the competence of the Drosophila female germline stem cell niche to respond to Notch ligands. *Dev. Biol.* **350**, 290-300.
Hsu, H.-J., LaFever, L. and Drummond-Barbosa, D. (2008). Diet controls normal and tumorous germline stem cells via insulin-dependent and -independent mechanisms in Drosophila. *Dev. Biol.* **313**, 700-712.
Issigonis, M. and Matunis, E. (2012). The Drosophila BCL6 homolog Ken and Barbie promotes somatic stem cell self-renewal in the testis niche. *Dev. Biol.* **368**, 181-192.
Jee, S. H., Kim, H. J. and Lee, J. (2005). Obesity, insulin resistance and cancer risk. *Yonsei Med. J.* **46**, 449-455.
Kai, T. and Spradling, A. (2003). An empty Drosophila stem cell niche reactivates the proliferation of ectopic cells. *Proc. Natl. Acad. Sci. USA* **100**, 4633-4638.
Kim, E., Goraksha-Hicks, P., Li, L., Neufeld, T. P. and Guan, K.-L. (2008). Regulation of TORC1 by Rag GTPases in nutrient response. *Nat. Cell Biol.* **10**, 935-945.
Kwak, S.-J., Hong, S.-H., Bajracharya, R., Yang, S.-Y., Lee, K.-S. and Yu, K. (2013). Drosophila adiponectin receptor in insulin producing cells regulates glucose and lipid metabolism by controlling insulin secretion. *PLoS ONE* **8**, e68641.
LaFever, L. and Drummond-Barbosa, D. (2005). Direct control of germline stem cell division and cyst growth by neural insulin in *Drosophila*. *Science* **309**, 1071-1073.
LaFever, L., Feoktistov, A., Hsu, H.-J. and Drummond-Barbosa, D. (2010). Specific roles of Target of rapamycin in the control of stem cells and their progeny in the *Drosophila* ovary. *Development* **137**, 2117-2126.
Laplante, M. and Sabatini, D. M. (2012). mTOR signaling in growth control and disease. *Cell* **149**, 274-293.
Lazareva, A. A., Roman, G., Mattox, W., Hardin, P. E. and Dauwalder, B. (2007). A role for the adult fat body in Drosophila male courtship behavior. *PLoS Genet.* **3**, e16.
Ma, X., Wang, S., Do, T., Song, X., Inaba, M., Nishimoto, Y., Liu, L.-p., Gao, Y., Mao, Y., Li, H. et al. (2014). Piwi is required in multiple cell types to control germline stem cell lineage development in the Drosophila ovary. *PLoS ONE* **9**, e90267.
Matsuoka, S., Hiromi, Y. and Asaoka, M. (2013). Egfr signaling controls the size of the stem cell precursor pool in the *Drosophila* ovary. *Mech. Dev.* **130**, 241-253.
McGuire, S. E., Le, P. T., Osborn, A. J., Matsumoto, K. and Davis, R. L. (2003). Spatiotemporal rescue of memory dysfunction in *Drosophila*. *Science* **302**, 1765-1768.
McMillan, D. C., Sattar, N. and McArdle, C. S. (2006). ABC of obesity. Obesity and cancer. *BMJ* **333**, 1109-1111.
Murguía, J. R. and Serrano, R. (2012). New functions of protein kinase Gcn2 in yeast and mammals. *IUBMB Life* **64**, 971-974.
Nässel, D. R. and Winther, A. M. (2010). *Drosophila* neuropeptides in regulation of physiology and behavior. *Prog. Neurobiol.* **92**, 42-104.
Natarajan, K., Meyer, M. R., Jackson, B. M., Slade, D., Roberts, C., Hinnebusch, A. G. and Marton, M. J. (2001). Transcriptional profiling shows that Gcn4p is a master regulator of gene expression during amino acid starvation in yeast. *Mol. Cell. Biol.* **21**, 4347-4368.
O'Brien, L. E., Soliman, S. S., Li, X. and Bilder, D. (2011). Altered modes of stem cell division drive adaptive intestinal growth. *Cell* **147**, 603-614.
Palanker, L., Tennessen, J. M., Lam, G. and Thummel, C. S. (2009). Drosophila HNF4 regulates lipid mobilization and beta-oxidation. *Cell Metab.* **9**, 228-239.
Rajan, A. and Perrimon, N. (2012). *Drosophila* cytokine unpaired 2 regulates physiological homeostasis by remotely controlling insulin secretion. *Cell* **151**, 123-137.
Reiher, W., Shirras, C., Kahnt, J., Baumeister, S., Isaac, R. E. and Wegener, C. (2011). Peptidomics and peptide hormone processing in the *Drosophila* midgut. *J. Proteome Res.* **10**, 1881-1892.
Rosen, E. D. and Spiegelman, B. M. (2014). What we talk about when we talk about fat. *Cell* **156**, 20-44.
Ruaud, A.-F., Lam, G. and Thummel, C. S. (2011). The Drosophila NR4A nuclear receptor DHR38 regulates carbohydrate metabolism and glycogen storage. *Mol. Endocrinol.* **25**, 83-91.
Rusten, T. E., Lindmo, K., Juhász, G., Sass, M., Seglen, P. O., Brech, A. and Stenmark, H. (2004). Programmed autophagy in the Drosophila fat body is induced by ecdysone through regulation of the PI3K pathway. *Dev. Cell* **7**, 179-192.

Development (2014) 141, 4479-4488 doi:10.1242/dev.116467

Sieber, M. H. and Thummel, C. S. (2009). The DHR96 nuclear receptor controls triacylglycerol homeostasis in Drosophila. *Cell Metab.* **10**, 481-490.

Slaidina, M., Delanoue, R., Gronke, S., Partridge, L. and Léopold, P. (2009). A Drosophila insulin-like peptide promotes growth during nonfeeding states. *Dev. Cell* **17**, 874-884.

Song, X., Call, G. B., Kirilly, D. and Xie, T. (2007). Notch signaling controls germline stem cell niche formation in the *Drosophila* ovary. *Development* **134**, 1071-1080.

Spradling, A. (1993). Developmental genetics of oogenesis. In *The Development of Drosophila melanogaster* (ed. M. Bate), pp. 1-70. Plainview, NY: Cold Spring Harbor Laboratory Press.

Sulkowski, M., Kim, Y.-J. and Serpe, M. (2014). Postsynaptic glutamate receptors regulate local BMP signaling at the *Drosophila* neuromuscular junction. *Development* **141**, 436-447.

Sun, P., Quan, Z., Zhang, B., Wu, T. and Xi, R. (2010). TSC1/2 tumour suppressor complex maintains *Drosophila* germline stem cells by preventing differentiation. *Development* **137**, 2461-2469.

Tapon, N., Ito, N., Dickson, B. J., Treisman, J. E. and Hariharan, I. K. (2001). The *Drosophila* tuberous sclerosis complex gene homologs restrict cell growth and cell proliferation. *Cell* **105**, 345-355.

Vucenik, I. and Stains, J. P. (2012). Obesity and cancer risk: evidence, mechanisms, and recommendations. *Ann. N. Y. Acad. Sci.* **1271**, 37-43.

Xie, T. and Spradling, A. C. (1998). decapentaplegic is essential for the maintenance and division of germline stem cells in the *Drosophila* ovary. *Cell* **94**, 251-260.

Xue, F. and Michels, K. B. (2010). Caloric restriction and cancer. In *Cancer and Energy Balance, Epidemiology and Overview* (ed. N. A. Berger), pp. 181-199. Springer: Heidelberg, Germany.

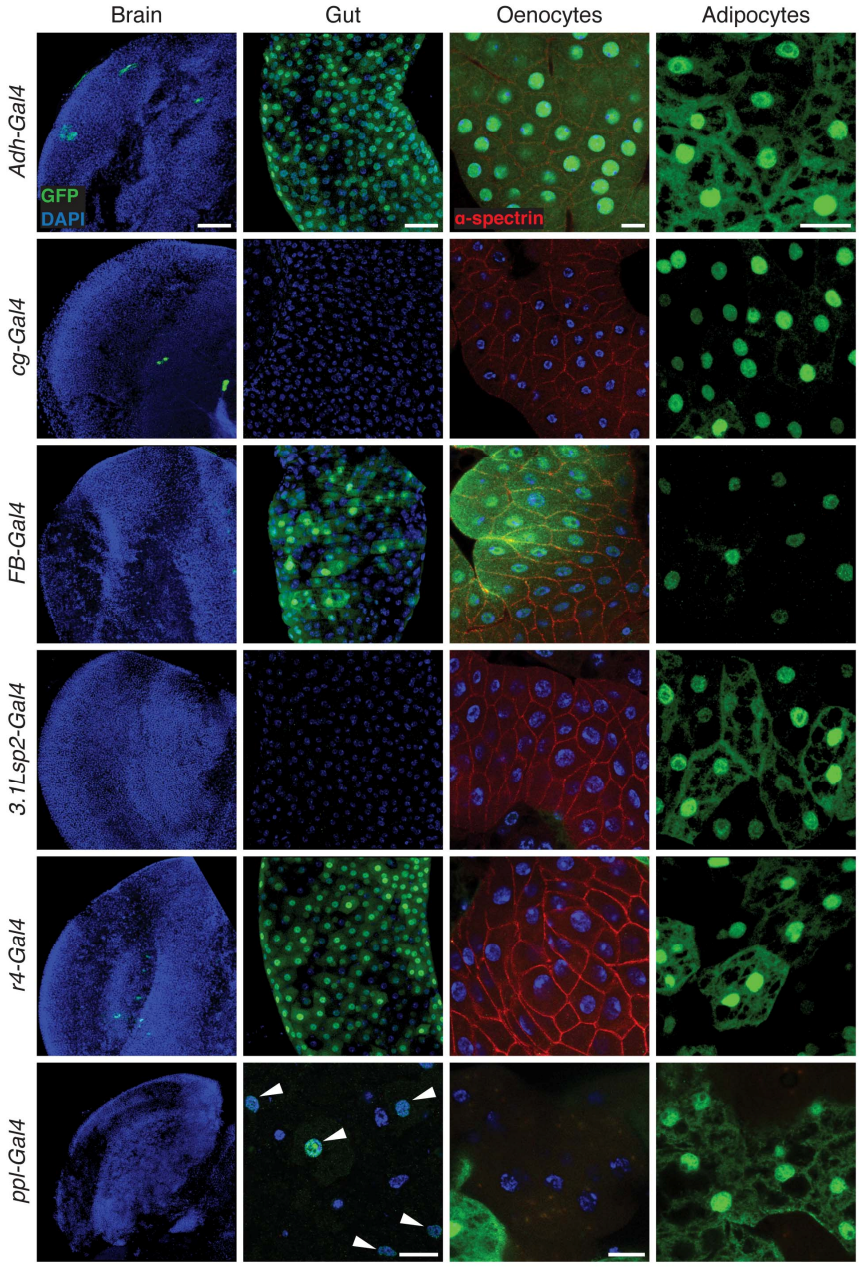

Fig. S1. In adult females, *3.1Lsp2-Gal4* is exclusively expressed in adipocytes. Expression of *UAS-GFP* (green) induced by several larval and/or adult fat body Gal4 drivers in adult female tissues shows that only *3.1Lsp2-Gal4* is exclusively expressed in adipocytes. DAPI (blue) labels nuclei in brains, guts and oenocytes; α-spectrin (red) labels cell membranes in

oenocytes (except in *ppl-Gal4*). Arrowheads indicate GFP-positive nuclei in the gut, for *ppl-Gal4*. Scale bars: 50 µm (brains), 50 µm (guts, for all except *ppl-Gal4*), 20 µm (gut, for *ppl-Gal4*), 10 µm (oenocytes), or 20 µm (adipocytes).

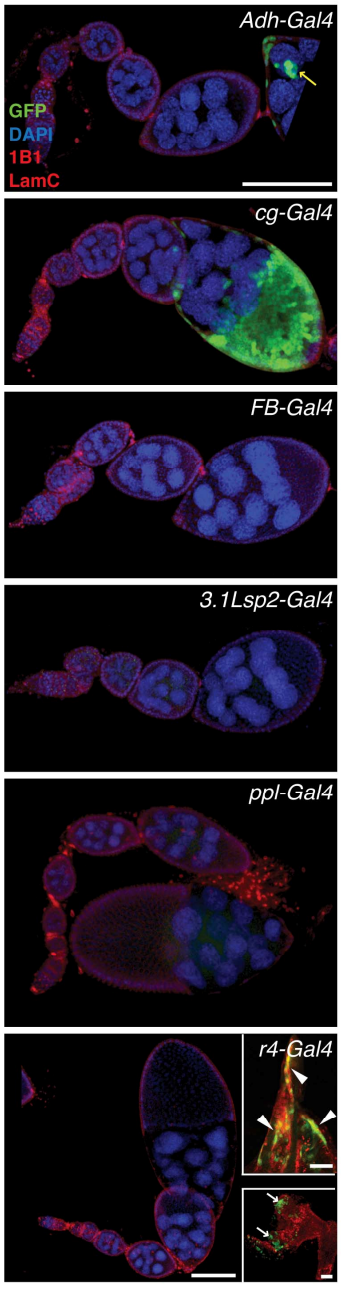

Supplemental Figure 2
Armstrong, Laws and Drummond-Barbosa

Fig. S2. *3.1Lsp2-Gal4* is not expressed in ovaries.

Analysis of *UAS-GFP* (green) induced by fat body Gal4 drivers shown in Figure 1 in adult ovaries shows that *3.1Lsp2-Gal4* has no ovarian expression. *Adh-Gal4* is expressed late follicle cells, including border cells (yellow arrow), *cg-Gal4* is expressed in stage 10 and later

follicle cells, and *r4-Gal4* is expressed in late dorsal-anterior follicle cells (arrowheads) and oviduct (white arrows). DAPI (blue) labels nuclei; 1B1 (red) labels cell membranes; LamC (red) labels nuclear envelopes of a subset of terminally differentiated cells. Scale bars: 100 μm (main panels), 50 μm (top inset), 50 μm (bottom inset).

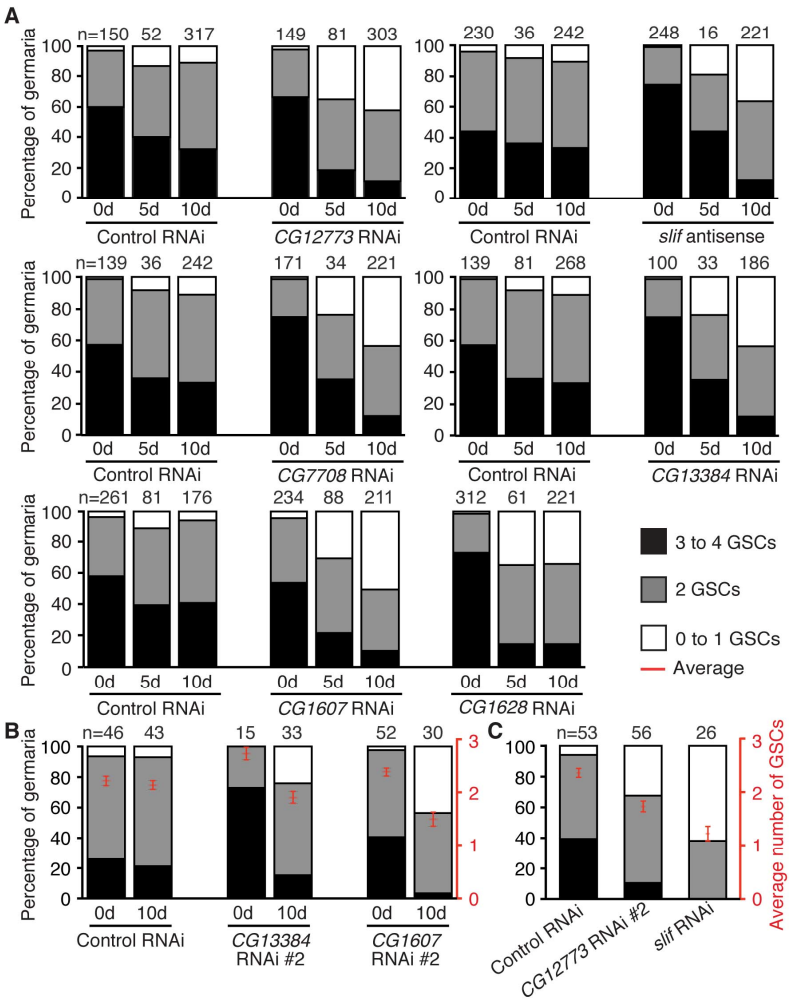

Supplemental Figure 3
Armstrong, Laws, and Drummond-Barbosa

Fig. S3. Reduced amino acid transport in adipocytes leads to higher rates of GSC loss in the ovary.

(**A-C**) Frequencies of germaria containing zero-or-one, two, or three-or-four GSCs at different days after switch to 29°C for *Gal80^{ts}; Lsp2*-mediated induction of a *UAS-slif*

antisense or *UAS-RNAi* transgenes against amino acid transporters *CG12773*, *CG7708*, *CG13384*, *CG1607*, *CG1628*, *CG12943* or *white* control. The same data used to calculate GSC number averages in Fig. 4 are plotted in (A). In (C), data at 10 days after switch to 29^{o}C are shown. The reduction in average GSC numbers upon adipocyte inhibition of amino acid transport (Fig. 4) reflects an increased percentage of germaria showing zero-or-one GSC and decreased fraction retaining two or three-or-four GSCs. The right *y*-axis in (B,C) shows the average number of cap cells per germarium. Number of germaria analyzed is shown above each bar.

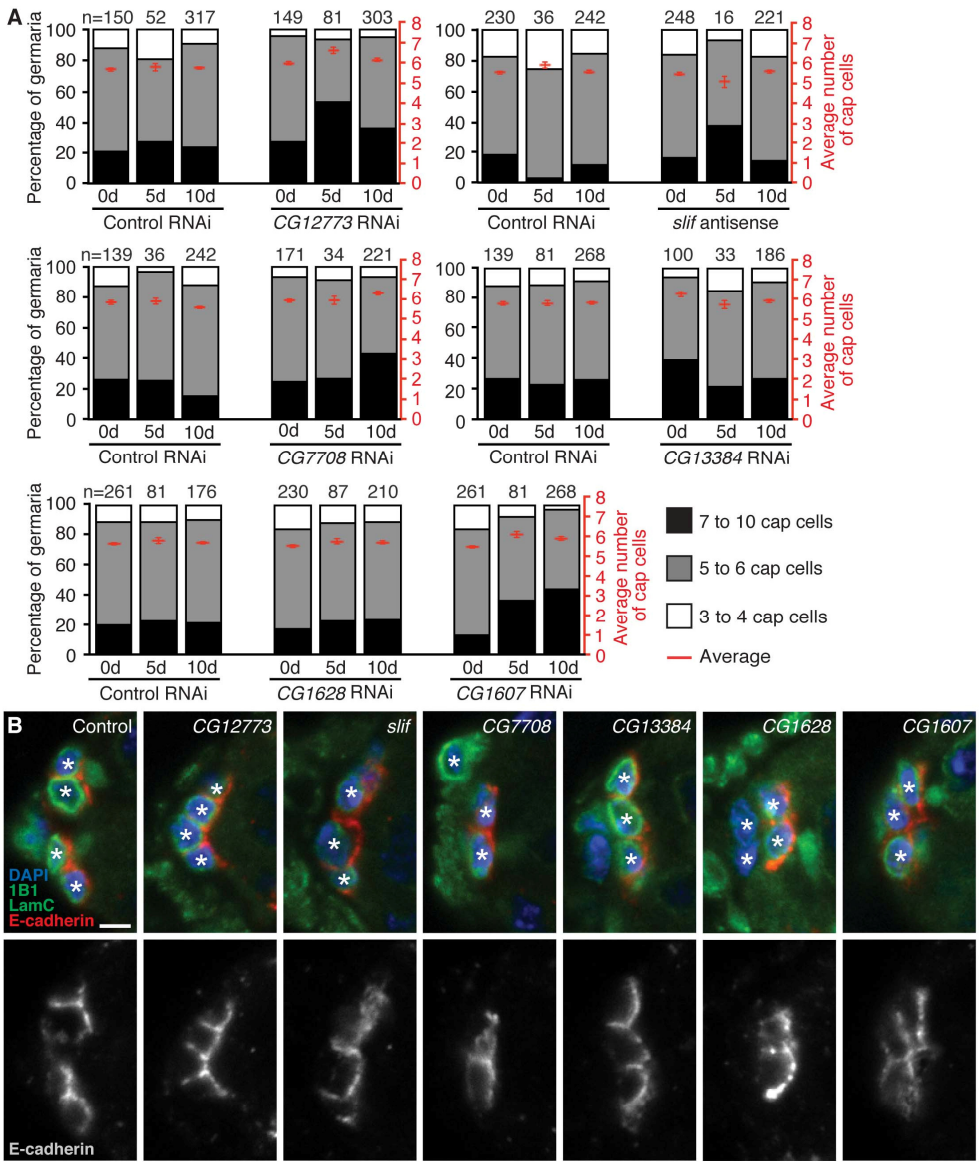

Supplemental Figure 4
Armstrong, Laws, and Drummond-Barbosa

Fig. S4. Reduced amino acid transport in adipocytes does not affect cap cell number or E-cadherin levels.

(**A**) Frequencies of germaria containing three-or-four, five-or-six, or seven-to-10 cap cells (left *y*-axis), and average number of cap cells per germarium (right *y*-axis) at different days

after switch to 29°C for *Gal80^{ts}; Lsp2*-mediated induction of a *UAS-slif antisense* or *UAS-RNAi* transgenes against amino acid transporters *CG12773*, *CG7708*, *CG13384*, *CG1607*, *CG1628*, *CG12943* or *white* control. Number of germaria analyzed is shown above each bar. (**B**) Germaria from females at 10 days of adult adipocyte-specific knockdown of amino acid transporters or *white* control gene showing no obvious difference in levels of E-cadherin (red) at GSC-cap cell junctions. DAPI (blue) labels nuclei; 1B1 (green) labels fusomes; LamC (green) labels cap cell nuclear envelopes. Asterisks indicate cap cells. Scale bar, 2.5 μm.

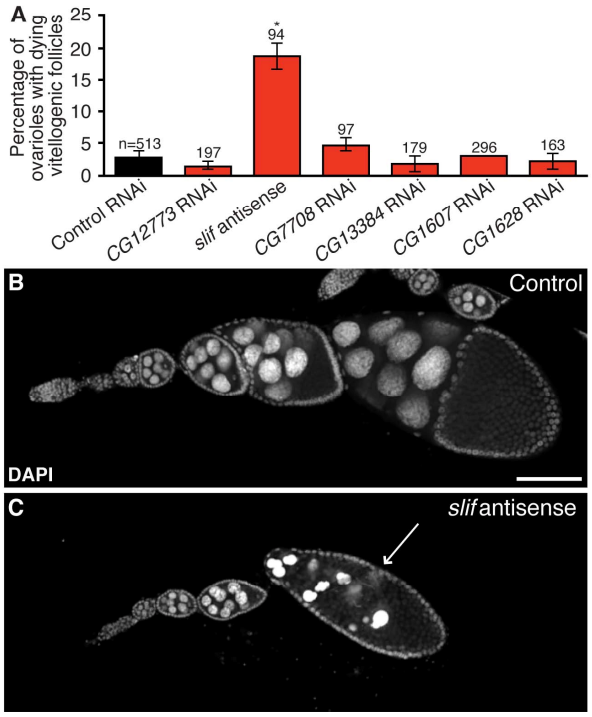

Supplemental Figure 5
Armstrong, Laws and Drummond-Barbosa

Fig. S5. Adult adipocyte-specific knockdown of amino acid transporters does not disrupt vitellogenesis, except in the case of *slif*.

(**A**) Percentage of ovarioles containing dying vitellogenic follicles at 10 days of adipocyte knockdown of amino acid transporters. Number of ovarioles analyzed is shown above each bar. **P*<0.05, Student's *t* test. Error bars indicate mean ± s.e.m. (**B,C**) DAPI-stained ovarioles from control (B) or *slif* (C) RNAi genotypes shown in (A). Arrow indicates degenerating follicle, recognized by the presence of pyknotic nuclei. Scale bar, 100 μm.

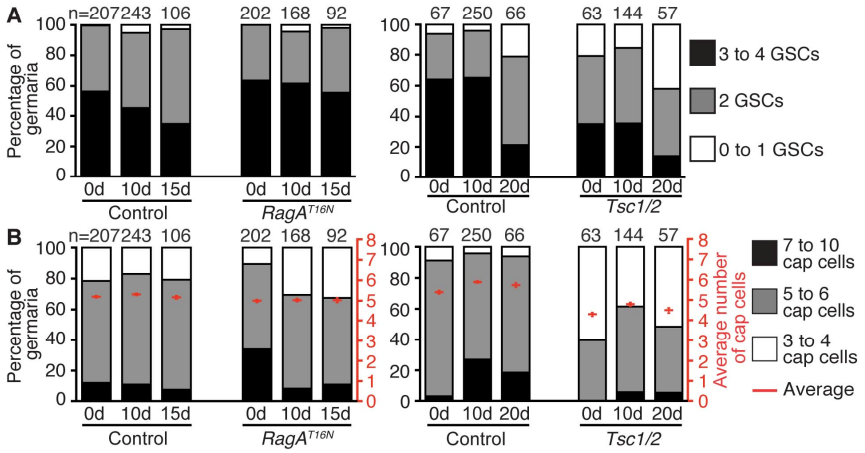

Supplemental Figure 6
Armstrong, Laws, and Drummond-Barbosa

Fig. S6. Reduced TOR signaling in adult adipocytes does not affect GSC or cap cell number.

(**A,B**) Frequencies of germaria containing zero-or-one, two, or three-or-four GSCs (A), or three-or-four, five-or-six, or seven-to-ten cap cells (B) at different days after switch to 29°C

for *Gal80^{ts}; Lsp2*-mediated induction of dominant negative *UAS-RagA^{T16N}* or *UAS-Tsc1* and *UAS-Tsc2* (*Tsc1/2*) transgenes. The same data used to calculate GSC number averages in Fig. 6A are plotted in (A). The right *y*-axis in (B) shows the average number of cap cells per germarium. Number of germaria analyzed is shown above each bar.

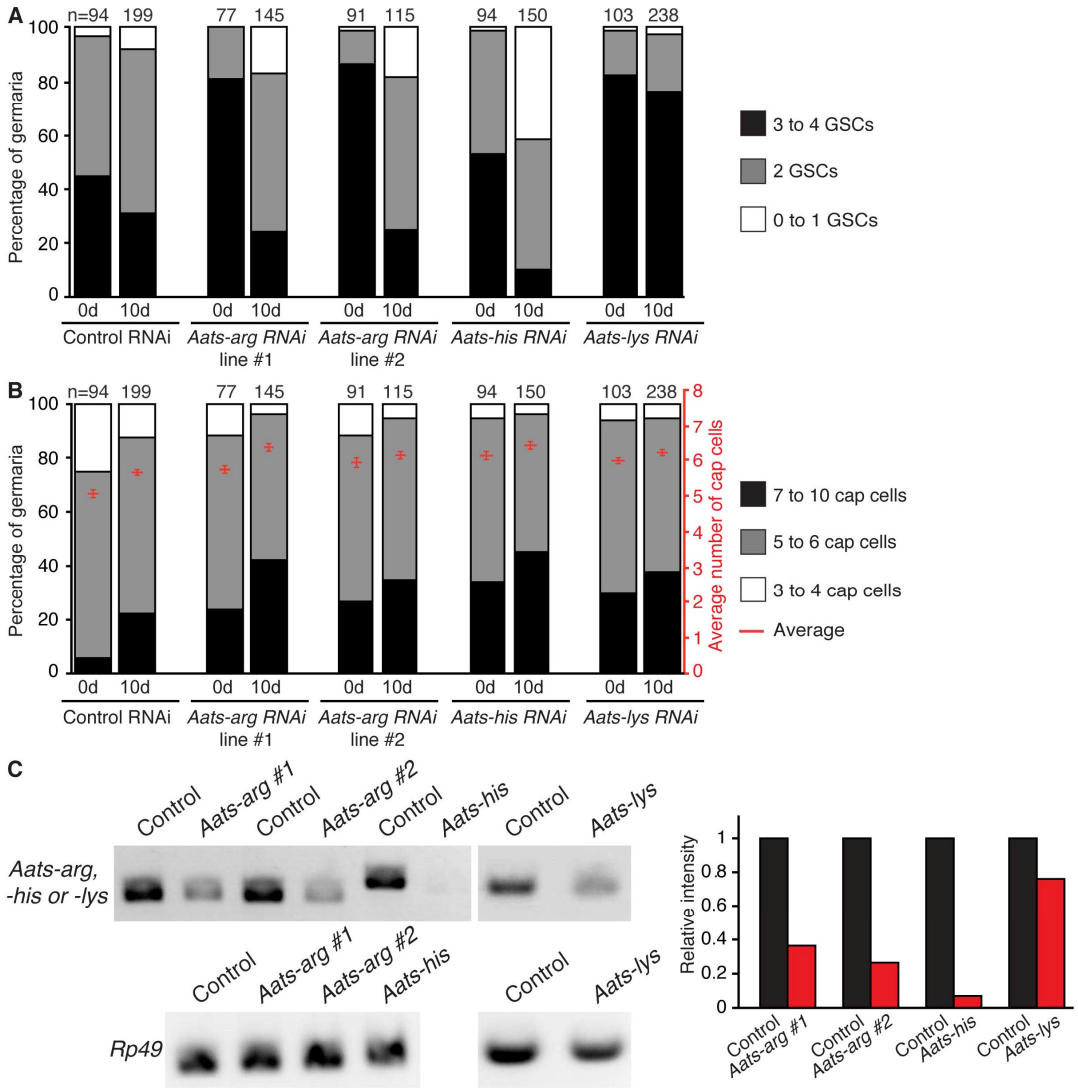

Supplemental Figure 7
Armstrong, Laws and Drummond-Barbosa

Fig. S7. Adult adipocyte-specific knockdown of aminoacyl-tRNA synthetases causes a reduction in GSC, but not cap cell, numbers.

(**A,B**) Frequencies of germaria containing zero-or-one, two, or three-or-four GSCs (A), or three-or-four, five-or-six, or seven-to-10 cap cells (B) at zero or 10 days after switch to 29°C

for *Gal80^{ts}; Lsp2*-mediated induction of *GFP* control, *Arginyl-tRNA synthetase* (*Aats-arg*), *Histidyl-tRNA synthetase* (*Aats-his*), or *Lysyl-tRNA synthetase* (*Aats-lys*) RNAi transgenes. The same data used to calculate GSC number averages in Fig. 7A are plotted in (A). The right *y*-axis in (B) shows the average number of cap cells per germarium. Number of germaria analyzed is shown above each bar. (**C**) RT-PCR analysis of hand-dissected fat bodies showing knockdown of amino acid transporters at 10 days of *Gal80^{ts}; Lsp2*-mediated induction of RNAi transgenes against *aminoacyl-tRNA synthetases* or *GFP* control. Note that *Aats-lys* knockdown was relatively inefficient and did not alter GSC number.

Table S1. Amino acid transporters tested in this study

AAT[a]	Type[b]	RNAi transgene #1	RNAi transgene #2[c]	Fat body expression[d]
CG1607[e]	polyamine transporter	*P{GD4651}v14925*	*P{KK107364}VIE-260B*	larval/adult
CG1628	L-ornithine transporter	*P{KK108506}VIE-260B*	*P{GD8885}v47475*	adult
CG4991	n.s.[f]	*P{GD3406}v30263*	-	-
CG5535	cationic amino acid transporter	*P{KK100907}VIE-260B*	-	-
CG7255	cationic amino acid transporter	*P{KK110010}VIE-260B*	-	-
CG7708	proline:sodium symporter; choline transporter	*P{KK109385}VIE-260B*	*P{GD3648}v30302*	-
CG7888	n.s.	*P{GD2411}v37263*	-	-
CG8785	n.s.	*P{GD1961}v4650*	-	-
CG9413	polyamine transporter	*P{KK101306}VIE-260B*	-	-
CG12531	polyamine transporter; cationic amino acid transporter	*P{KK109373}VIE-260B*	-	-
CG12773	sodium:potassium: chloride symporter	*P{KK102472}VIE-260B*	*P{GD3189}v9899*	larval/adult
CG12943	n.s.	*P{KK112469}VIE-260B*	-	-
CG13248	polyamine transporter; cationic amino acid transporter	*P{KK103406}VIE-260B*	-	-
CG13384	n.s.	*P{KK102447}VIE-260B*	*P{GD1007}v44246*	adult
CG13646	n.s.	*P{GD257}v1571*	-	-
CG13743	n.s.	*P{GD3488}v40974*	-	-
CG16700	GABA:hydrogen symporter	*P{GD3405}v45188*	-	-
CG17119	L-cystine transporter	*P{GD3122}v51127*	-	-
CG30394	n.s.	*P{GD2127}v3470*	-	-
CG32079	n.s.	*P{KK107121}VIE-260B*	-	-
dmGlut	glutamate transporter	*P{TRiP.HMS01615}attP2*	-	larval
kazachoc	potassium:chloride symporter activity	*P{TRiP.HMS01058}attP2*	-	-
minidiscs	polyamine transporter; leucine import	*P{GD453}v42485*	-	adult[g]
Ncc69	sodium:potassium:chloride symporter	*P{KK108763}VIE-260B*	-	-
pathetic	n.s.	*P{KK104735}VIE-260B*	-	larval
slimfast	polyamine transporter; cationic amino acid transporter	*slif antisense*[h]	*P{GD12619}v45590*	larval[h]

[a] AAT, amino acid transporter. The *Drosophila* genome encodes 40 predicted amino acid transporters; for 26 of them, RNAi lines were available (www.flybase.org).
[b] Type of amino acid transporter according to FlyBase annotation (www.flybase.org).
[c] The second set of RNAi lines target sequences that are different from those targeted by the first set (stockcenter.vdrc.at).
[d] Fat body expression is listed as reported in FlyBase, except where indicated.
[e] The red font indicates amino acid transporters followed up on in this study.
[f] n.s., not specified.
[g] Adult fat body expression of *minidiscs* reported in Martin et al., 2000.
[h] Larval fat body expression of *slif* and *UAS-slif* antisense transgene described in Colombani et al., 2003.

Table S2. Primers used for RT-PCR analyses

Gene	Forward	Reverse
CG1607	DDB788 (5'-AGTATCGGTGTGGCTGTATTG-3')	DDB789 (5'-CTGGCAGAAGTTGTTGTGTATTT-3')
CG12773	DDB763 (5'-CATGTTAATGCCCGACAG-3')	DDB764 (5'-CATAGCTCTCGTCAGCGTC-3')
CG13384	DDB790 (5'-CTGGATCGGGAGATGATGAAAT-3')	DDB791 (5'-ACGCCACAAAGAGGAAGTAG-3')
Aats-arg	DDB796 (5'-CCGAACGATCTGCTATCCTAAA-3')	DDB797 (5'-TCTTAGCCAGCTTCCATTCC-3')
Aats-his	DDB794 (5'-CCACATCGCCAAGGTCTATC-3')	DDB795 (5'-ATCGAAGCTAACTCGCTTATCC-3')
Aats-lys	DDB792 (5'-GGCTCCTACAAGGTCATCTATC-3')	DDB793 (5'-GGTATACGCGTTGCAAATCTC-3')
Gcn2	DDB811 (5'-ACACTGGCCCTAAGCCAATC-3')	DDB812 (5'-GCCTTGCTGGTGAATATGCG-3')
Rp49	DDB137 (5'-CAGTCGGATCGATATGCTAAGC-3')	DDB138 (5'-AATCTCCTTGCGCTTCTTGG-3')